Cell Transplantation, Vol. 19, pp. 313–328, 2010

0963-6897/10 $90.00 + .00
DOI: 10.3727/096368909X480323
E-ISSN 1555-3892
www.cognizantcommunication.com

Transplantation of Mesenchymal Stem Cells Exerts a Greater Long-Term Effect Than Bone Marrow Mononuclear Cells in a Chronic Myocardial Infarction Model in Rat

Manuel Mazo,* Juan José Gavira,† Gloria Abizanda,* Cristina Moreno,‡ Margarita Ecay,§ Mario Soriano,# Pablo Aranda,* María Collantes,§ Eduardo Alegría,† Juana Merino,‡ Iván Peñuelas,¶ José Manuel García Verdugo,# Beatriz Pelacho,*[1] and Felipe Prósper*[1]

*Hematology and Cell Therapy and Division of Cancer, Clinica Universitaria and Foundation for Applied Medical Research, University of Navarra, Navarra, Spain
†Department of Cardiology and Cardiovascular Surgery, University of Navarra, Navarra, Spain
‡Immunology Service, University of Navarra, Navarra, Spain
§MicroPET Research Unit CIMA-CUN, University of Navarra, Navarra, Spain
¶Radiopharmacy Unit, Department of Nuclear Medicine Clínica Universitaria, University of Navarra, Navarra, Spain
#Department of Cell Biology, Instituto Cavanilles, University of Valencia, Valencia, Spain

The aim of this study is to assess the long-term effect of mesenchymal stem cells (MSC) transplantation in a rat model of chronic myocardial infarction (MI) in comparison with the effect of bone marrow mononuclear cells (BM-MNC) transplant. Five weeks after induction of MI, rats were allocated to receive intramyocardial injection of 10^6 GFP-expressing cells (BM-MNC or MSC) or medium as control. Heart function (echocardiography and ^{18}F-FDG-microPET) and histological studies were performed 3 months after transplantation and cell fate was analyzed along the experiment (1 and 2 weeks and 1 and 3 months). The main findings of this study were that both BM-derived populations, BM-MNC and MSC, induced a long-lasting (3 months) improvement in LVEF (BM-MNC: $26.61 \pm 2.01\%$ to $46.61 \pm 3.7\%$, $p < 0.05$; MSC: $27.5 \pm 1.28\%$ to $38.8 \pm 3.2\%$, $p < 0.05$) but remarkably, only MSC improved tissue metabolism quantified by ^{18}F-FDG uptake (71.15 ± 1.27 to 76.31 ± 1.11, $p < 0.01$), which was thereby associated with a smaller infarct size and scar collagen content and also with a higher revascularization degree. Altogether, results show that MSC provides a long-term superior benefit than whole BM-MNC transplantation in a rat model of chronic MI.

Key words: Bone marrow stem cells; Chronic myocardial infarction; Cardiac remodeling; Angiogenesis

INTRODUCTION

Cardiovascular diseases are a leading health concern in Western countries (40), with ischemia as the main mechanism for loss of cardiomyocyte (CM) mass and contractile force. In spite of new approaches and therapies (9,22,25,26,34,39,57), regeneration of the damaged tissue has not been successfully achieved, and compensation of chronic hypertrophy is in most cases difficult, leaving heart transplantation as the only alternative for end-stage patients.

Stem cell application to the field of regenerative medicine offers new strategies to induce tissue repair and the potential for improvement in cardiac function. Different cell types (51) have been employed in animal models [reviewed in (53)] with, importantly, bone marrow-mononuclear cells (BM-MNC) (37), mesenchymal stem cells (21), and skeletal myoblasts undergoing clinical trials (3,35,42,45). Although animal studies and phase I studies suggested a positive effect of these cell populations, recently published randomized clinical trials have shown controversial results (42,43). Although new long-term studies with larger patient groups are required in order to confirm these data, the use of other cell types that could offer better chances to regenerate the infarcted heart may be a useful approach.

Received April 15, 2009; final acceptance November 10, 2009. Online prepub date: November 16, 2009.
[1]B.P. and F.P. contributed equally to this work and should be considered equal last authors.
Address correspondence to Felipe Prósper, M.D., Hematology and Cell Therapy, Clínica Universitaria, Av. Pío XII 36, Pamplona 31008, Navarra, Spain. Tel: 34 948 255400; Fax: 34 948 296500; E-mail: fprosper@unav.es *or* Beatriz Pelacho, Ph.D., Foundation for Applied Medical Research, Av. Pío XII 57, Pamplona 31008, Navarra, Spain. Tel: 34 948 194700; E-mail: bpelacho@unav.es

Bone marrow has been shown to contain several populations of stem cells like hematopoietic stem cells, endothelial progenitor cells, mesenchymal stem cells (MSC) [reviewed in (32)], and others with greater differentiation capacity like the multipotent adult progenitor cells (MAPC) (24), the marrow-isolated multilineage inducible (MIAMI) cells (13), or the very small embryonic-like (VSEL) cells (30). While the product obtained from a bone marrow aspiration contains some of these progenitors, their proportion might be too low to exert any significant benefit in the setting of cardiac ischemia. It is thus logical to believe that enrichment of some of these populations in vitro could enhance the beneficial effects of BM-MNC transplantation. On the other hand, MSC have attracted much attention in the field given their potential to transdifferentiate into suitable phenotypes (17,19,36) and also to exert paracrine actions upon the ischemic tissues (29,38). Moreover, their immunomodulatory properties (31) could exert a positive effect after transplantation into the heart by regulation of tissue inflammation (4). On top of this, their in vitro processing is simple and even in humans renders sufficient amount of cells for an optimum treatment of the disease.

Currently, although many studies have been performed with different stem cell preparations in myocardial ischemia models, the lack of comparative studies makes it difficult to determine which population has a better regenerative effect. Moreover, bone marrow-derived stem cells have been mainly tested in acute models of myocardial infarction. Thus, in the current study we sought to compare the long-term putative beneficial effects of two stem cell populations derived from the BM: freshly isolated BM-MNC and bone marrow MSC in a chronic model of myocardial infarction.

MATERIALS AND METHODS

Isolation and Characterization of Cells

All eGFP cells (bone marrow) were isolated from 4–6-week-old Sprague-Dawley eGFP rats. Bone marrow cells were harvested from rat femurs and isolated by means of a Ficoll-Paque density gradient centrifugation. For BM-MNC transplantation, cells were washed and resuspended in culture media (DMEM, Invitrogen, Leiden, The Netherlands) without supplements at a concentration of 10^6 cells in 70 μl. Viability by trypan blue dye exclusion was shown to be above 98%.

MSC were obtained from mononuclear cells. Briefly, cells were seeded at 50,000 cells/cm^2 in αMEM (Invitrogen) with 10% fetal calf serum (FCS, Cambrex, Milano, Italy), 1% penicillin/streptomycin, and 10 ng/ml bFGF (Sigma, Madrid, Spain) and maintained in a humidified atmosphere in 5% CO_2. Subconfluent MSC were obtained within a week and passed at 5000 cells/cm^2. Cells were used for transplant after five passages. Characterization of MSC was performed by FACS and differentiation capacity. Cells were stained with antibodies against RT1A, RT1B, CD31, CD44, CD45, CD73, and CD90 (all purchased from BD, Madrid, Spain). For osteogenic differentiation, cells were plated at 6000 cells/cm^2 in osteogenic media [αMEM with 10% FCS, 1% antibiotics, 10 mM β-glicerolphosphate (Sigma), 0.2 mM ascorbate-2-phosphate (Sigma), and 0.01 μM dexamethasone (Sigma)]. Condrogenic differentiation was performed with 200,000 pelleted cells suspended in condrogenic media [DMEM-high glucose (Invitrogen) with 1% antibiotics, 10 ng/ml TGF-β3 (R&D Systems, Minneapolis, MN, USA), 50 mg/ml ITS+Premix (BD), 40 μg/ml proline (Sigma), 500 ng/ml BMP6 (R&D Systems), 50 μg/ml ascorbate-2-P, and 0.1 μM dexamethasone]. For adipogenic differentiation, when cells reached 95–100% confluence, expansion media was replaced with adipogenic media [αMEM with 10% FCS, 1% antobiotics, 50 μM indomethacin (Sigma), 0.5 mM IBMX (Sigma), and 1 μM dexamethasone]. All differentiation protocols were maintained for 21 days. Analysis of cell differentiation was performed by histochemical staining by Oil red O (adipogenic), Alizarin red (osteogenic), and toluidine blue (condrogenic) following previously described protocols (62).

Experimental Model

A total of 115 female Sprague-Dawley rats (Harlan IBERICA S.L. Barcelona, Spain) underwent coronary artery ligation of the left coronary artery as previously described (3). Only those animals that survived ($n = 97$) and with a LVEF below 40% at 1 month post-MI were included in the study ($n = 75$). Five weeks after myocardial infarction induction, rats were reoperated by sternotomy and allocated to receive 10^6 cells per animal (total volume: 70 μl) of BM-MNC ($n = 24$), MSC ($n = 25$), or control medium ($n = 26$) in two points of the infarct border region. Due to the allogeneic origin of the cells, animals were daily immune-suppressed with cyclosporin A (20 mg/kg/day, IP, Sandimmun, Novartis) from 2 days pretransplantation until sacrifice. Rate of survival over the course of the experiment was over 98%. All experiments, including bone marrow cell isolation, were performed in accordance with the principles of laboratory animal care formulated by the National Society for Medical Research and the guide for the care and use of laboratory animals by the Institute of Laboratory Animal Resources (Commission on Life Science, National Research Council). All animal procedures were approved by the University of Navarra Institutional Committee on Care and Use of Laboratory Animals.

Tissue Processing and Staining

For histological analysis, three animals per group were sacrificed at 1, 2, and 4 weeks, respectively and

eight animals per group at 3 months. After sacrifice, rat hearts were excised, fixed in 4% paraformaldehyde for 4 h at 4°C, and cut in three equal size blocks (apical, midventricular, and basal). Hearts were either dehydrated in ethanol 70% (4°C o/n) and embedded in paraffin or saturated in 25% sucrose (4°C o/n), embedded in O.C.T. compound, and snap frozen in nitrogen-cooled isopentane. For histological analysis 5-μm sections were cut. Cell detection was based upon the presence of GFP-positive signals by inmunohistochemical [anti-GFP polyclonal Ab (pAb, Invitrogen) or anti-GFP raised in chicken pAb (Abcam, Cambridge, UK) diluted 1:500 in TBS] or immunofluorescence methods. For immunofluorescence, a tyramide amplifying kit (Invitrogen) or a secondary antibody anti-chicken IgY coupled to 655 nm emitting quantum dots were used following manufacturer's instructions. Immunolabeling was performed with antibodies against α-smooth muscle actin (α-SMA) [mouse monoclonal antibody (mAb) diluted 1:1000 in TBS; Sigma, Madrid, Spain] coupled to Cy3, cardiac troponin T (cTT) (mAb, diluted 1:100 in TBS; Labvision), ventricular myosin (mAb diluted 1:2 in TBS; BioCytex), Ki-67 (mAb, diluted 1:25 in TBS; DAKO, Barcelona, Spain), PCNA (mAb, diluted 1:100 in PBS; Santa Cruz), CD68 (mAb, diluted 1:200 in TBS; Serotec, Oxford, UK), caveolin-1 (mAb, diluted 1:100 in TBS, BD), connexin 43 (pAb, diluted 1:200 in TBS, Sigma). Secondary antibodies labeled with AlexaFluor-594 or AlexaFluor-488 were purchased from Molecular Probes (Invitrogen) if needed and used following the manufacturer's instructions. EnVision™-HRP conjugated system (Dako) was used as secondary reagent for immunohistochemistry. For nuclear staining, TOPRO-3 (diluted 1:50 in PBS-glycerol) for confocal microscopy or DAPI (diluted 1:4 in PBS-glycerol) for conventional IF microscopy were utilized. For confocal microscopy, a LSM 510 META (Carl Zeiss, Minneapolis, USA) microscope was used.

For Sirius Red staining, sections were deparaffinized and immersed in Sirius Red (Sigma) for 90 min, differentiated 2 min in HCl (Sigma) 0.01 N, dehydrated, and mounted in DPX. Hematoxylin-eosin staining was performed as detailed elsewhere (16). Briefly, sections where stained in Ehrlich's hematoxylin (Sigma) for 7 min, differentiated through water-HCl and Li_2CO_3 solutions, immersed in eosin (Sigma) for 10 s, dehydrated, and mounted in DPX.

Electron Microscopy

For electron microscopy studies, six to eight animals per group were sacrificed and hearts were fixed with 4% paraformaldehyde 0.5% glutaraldehyde. Sections were postfixed with 1% osmium (30 min), rinsed, dehydrated, and embedded in araldite (Durcupan, Fluka). Semithin sections (1.5 μm) were cut with a diamond knife and stained lightly with 1% toluidine blue. Later ultrathin (0.05 μm) sections were cut with a diamond knife, stained with lead citrate, and examined under a Fei Tecnai spirit electron microscopy. Over 15 samples per animal were analyzed.

Morphometric Analysis

Quantification of vascular density was performed in animals sacrificed 3 months posttransplantation. For capillary density (capillaries/mm^2), a total of 15 serial sections including the infarct area, 30 μm apart, were stained with caveolin-1 and a total of 30 infarct border images were analyzed. Arteriolar density (arterioles/mm^2) and arteriolar area (μm^2) were quantified in a similar way after staining with anti-α-SMA-Cy3 in the following sections. Pictures were taken on a Nikon Eclipse E800 microscope equipped with epifluorescence optics and digital images were analyzed using imaging software (Jay Image), or on a Zeiss LSM 510 META laser confocal microscope. The degree of fibrosis was determined by quantification of collagen deposition stained by Sirius red as previously described (16). Briefly, a mean of 15 serial sections were stained, each 30 μm apart. Infarct size was assessed as the mean percent of infarcted area versus total LV area, whereas fibrosis was measured in high-power photographs within the infarct as percent of collagen area (red) versus total tissue area using AnalySIS^R software. Cell engraftment was quantified after GFP immunostaining. Positive cells were only counted if their nucleus was identifiable. Tissue sections were screened and GFP cells quantified from the first to the last section with engrafted cells. This was made relative to the quantity of injected cells (10^{6M}) as the percentage of surviving cells.

Macrophage density was measured as number of CD68-positive cells per area unit in a mean of 15 sections, each 30 μm apart. Finally, cell proliferation was quantified in animals sacrificed 1 and 2 weeks after cell injection by counting PCNA-positive cells in sections stained for GFP, PCNA, and a lineage-specific marker, either caveolin-1 for endothelium or α-SMA for myofibroblast or smooth muscle. Number of sections was the same as for macrophage density. All photographs were taken on a Zeiss LSM 510 META laser confocal microscope.

Echocardiographic Studies

Animals were slightly anesthetized prior to study with 2% isoflurane (Forane®, Lab. ABBOTT S.A, Madrid, Spain) in 100% O_2 gas and placed in the supine or lateral position on a warming pad for transthoracic two-dimensional echocardiography, M-mode recordings, and Doppler ultrasound measurements as previously described (3). Echocardiography was performed using a Sonos 4500 ultrasound system (Philips) with a 12 MHz

linear array transducer and Doppler measurement. Left ventricular remodeling was assessed by measuring end systolic and diastolic volumes and diameters according to the American Society of Echocardiology. The left ventricular ejection fraction was determined in parasternal short axes (41) and diastolic function was assessed by measuring E and A waves of the mitral filling pattern by pulsed echo-Doppler technique in four-chamber apical views. Echocardiographic studies were performed at baseline (before infarct), before cell transplantation, and at day 90 posttransplant by the same blinded investigator. Measurements were done in three cycles and the mean value was obtained.

^{18}F-FDG PET Imaging Protocols, Image Reconstruction, and Semiquantitative Evaluation

Immediately before injection of cells and 90 days later, animals were subjected to PET analysis using the technique previously described by our group demonstrating that ^{18}F-FDG-micro-PET provides valuable semiquantitative information and allow noninvasive follow-up of heart glucose metabolism, representing a useful strategy for assessment of novel therapies in cardiac regeneration (49). Rats were anesthetized with 2% isoflurane in 100% O_2 gas and after tail vein injection of ^{18}F-FDG (75 MBq in 100–200 μl), immediately awakened, and placed back in the cage. Two hours after tracer injection, animals were anesthetized with isoflurane, placed prone on the PET scanner cradle, and kept during the overall study under continuous influx of the anesthetic. A static 60-min study (sinogram) was acquired in a Mosaic (Philips) small-animal dedicated imaging tomograph. Scanner efficiency normalization, dead time, and decay corrections were applied during reconstruction. Images were reoriented for further processing and polar maps obtained using the specific cardiac imaging software package of the PET scanner. After reorientation of transaxial images into short- and long-axis slices polar maps were generated and divided into 17 different ROIs. Individual quantification of the ^{18}F-FDG uptake in each of them was calculated. The total number of counts obtained for each of the ROIs was divided by its corresponding area to obtain counts per area unit. For each PET study, the maximal value of the 17 ROIs was considered as 100% and the remaining data transformed into percentage values. All further calculations and statistical analysis were performed on these sets of rescaled numerical data.

Statistical Analysis

All data are expressed as mean ± SEM or median (Q25; Q75). Comparisons for repeated measurements were performed by ANOVA accompanied by Tukey's HDS for intergroup comparisons or Kruskal-Wallis and Mann-Whitney test with Finner's correction of significance. Shapiro-Wilk test was used to verify that the data had a Gaussian distribution, which justifies the use of a parametric test. Statistical analysis was performed with the SPSS 11.0 software and differences were considered statistically significant when $p < 0.05$.

RESULTS

Cell Culture and Characterization

MSC presented a typical spindle-shape in culture conditions. GFP expression was monitored during culture and before transplantation, ensuring that over 90% of the cells were positive (not shown). At passage 4, this population had a FACS expression profile as follows: RT1A, CD44, CD73, and CD90 positive and RT1B, CD31, and CD45 negative (Fig. 1A, representative histograms are shown). Moreover, MSC differentiated towards condrogenic, adipogenic, and osteogenic lineages (Fig. 1B), thus proving their multipotency. BM-MNC were obtained following previously reported protocols (48).

Mesenchymal Cell Injection Induces a Long-Lasting Improvement of Cardiac Function and Tissue Metabolism

In order to assess if cell therapy was capable of inducing a long-lasting improvement in a model of rat chronic MI, cardiac function and tissue metabolism were monitored by echocardiography and microPET, 3 months after injection of BM-MNC, MSC, or control media. Artery ligation provoked a marked reduction of the left ventricular ejection fraction (LVEF) from baseline (72.23 ± 8.47%, mean ± SD) to preinjection (5 weeks later) (27.82 ± 6.69%), which did not differ between all three groups. Compared to their preimplant values, both BM-MNC and MSC treatment induced a statistically significant improvement of left ventricular (LV) function (BM-MNC: 26.61 ± 2.01% to 42.61 ± 3.7%; MSC: 27.5 ± 1.28% to 38.8 ± 3.2% pretransplant and 3 months, respectively; $p < 0.05$), whereas animals injected with medium did not show any improvement in the cardiac function (29.87 ± 2.84% to 28.1 ± 1.59%) (Fig. 2). No significant differences were detected between both cell-treated groups (BM-MNC vs. MSC; $p = 0.97$), indicating no superior benefit from one or the other cell population. Analysis of polar maps including the whole left ventricle (the 17 cardiac segments) showed that MSC-treated animals had a significant improvement in cardiac metabolism compared with their preinjection parameters (72.15 ± 1.17% to 76.31 ± 1.1%; $p < 0.01$) (Fig. 3A). MSC treatment proved to have a positive effect not only in global tissue metabolism, but more importantly when the analysis was restricted to the infarcted segments (7,

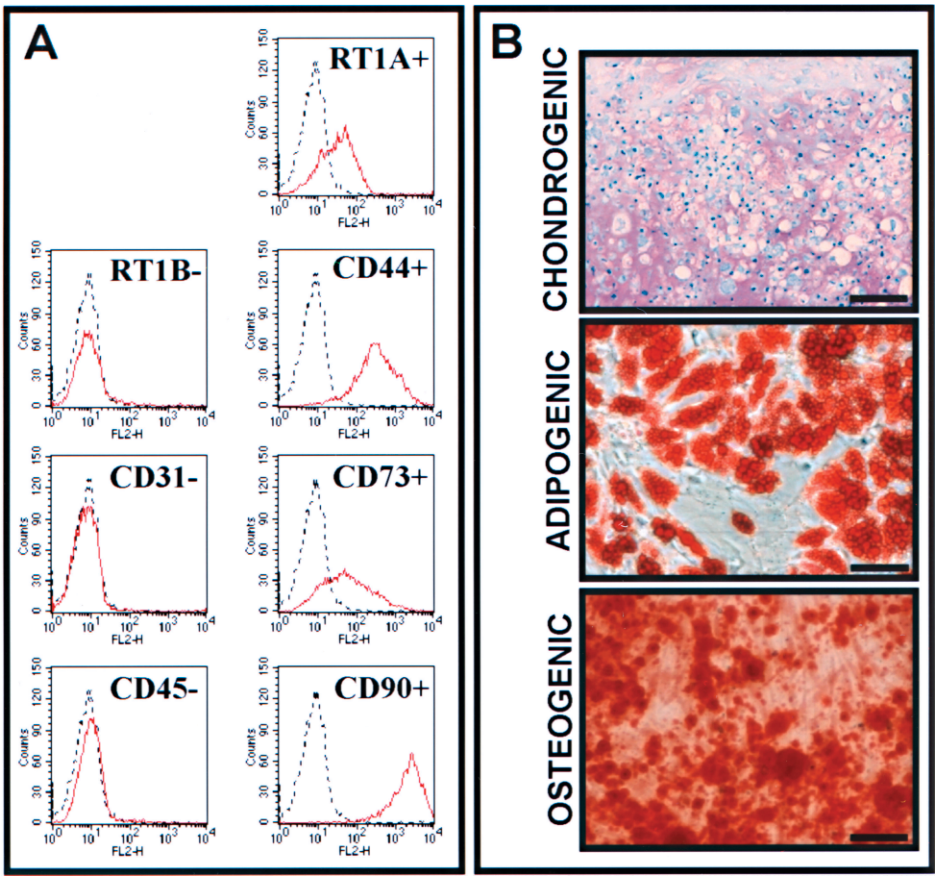

Figure 1. MSC characterization. (A) MSC were stained with antibodies against RT1B, CD31, CD45, RT1A, CD44, CD73, and CD90 (red line) or isotype controls (dashed line). (B) MSC were differentiated in vitro towards chondrocites (as shown by toluidine blue staining), adipocytes (Oil red O staining), and osteocytes (Alizarin red staining). Scale bars: 25 μm.

13, 16, and 17) as depicted by the significant increase in their metabolism (46.8 ± 3.35% to 53.02 ± 3.55%, $p < 0.05$) (Fig. 3B, C). On the contrary, BM-MNC injection did not have a significant effect in tissue metabolism (all segments: 70.87 ± 1.88% to 73.55 ± 1.88%; infarcted segments: 44.8 ± 4.3% to 50.4 ± 4.63%).

MSC Engraft in the Ischemic Tissue and Induce a Reduced Inflammatory Reaction Than BM-MNC

Cell fate was analyzed by immunohistochemical and immunofluorescence detection of GFP-positive cells at 1 and 2 weeks and 1 and 3 months after their transplantation in the border zone of the infarct. We found large patches of GFP-positive cells at the injection site in rats treated with MSC 1 and 2 weeks after transplantation, but not from 1 month onwards (Fig. 4A–D). Cell engraftment was quantified in MSC-treated animals as described in Materials and Methods. One week after transplant, 1.85% (0.53; 3.02) [median (Q25; Q75)] of the total number of injected cells were still present in the myocardium of infarcted animals, and this number decreased to 1.33% (0.52; 2.14) at 2 weeks, were almost not detectable at 1 month, and disappeared at 3 months. On the other hand, presence of GFP-BM-MNC could not be detected even at 1 week posttransplant (Fig. 4E–H). No positive signal was found on medium-injected animals (Fig. 4I–L).

It is possible that, despite immunosuppression, the GFP antigen could be recognized by the macrophages, which in turn could react against the transplanted cells (33). In order to study this, CD68 immunostaining was performed in animals sacrificed 1 week after transplant. Intra- and peri-infarct sections were analyzed and, as depicted in Figure 5, a strong macrophage infiltration was found in BM-MNC-treated animals, both in the infarct (327.6 ± 49.67 positive cells/mm^2, $p < 0.01$ vs. medium) (Fig. 5A–D) and peri-infarct (1945.78 ± 372.08 positive cells/mm^2, $p < 0.01$ vs. medium) (Fig. 5E–H) regions in comparison with media-injected animals (Medium, intra-infarct: 94.5 ± 6.05 positive cells/mm^2; peri-infarct:

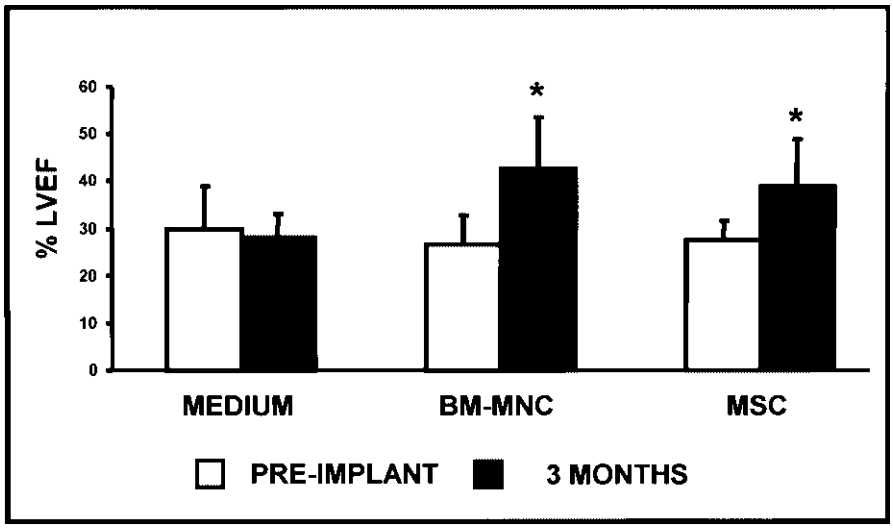

Figure 2. BM-MNC and MSC improve cardiac function. LVEF was assessed by echocardiography before and 3 months after transplantation of BM-MNC or MSC. Cell culture medium was injected in the control group. Results are shown as mean ± SD and statistical significance was calculated by comparing the LVEF values 3 months after transplantation versus preimplantation, in each group (*$p < 0.05$).

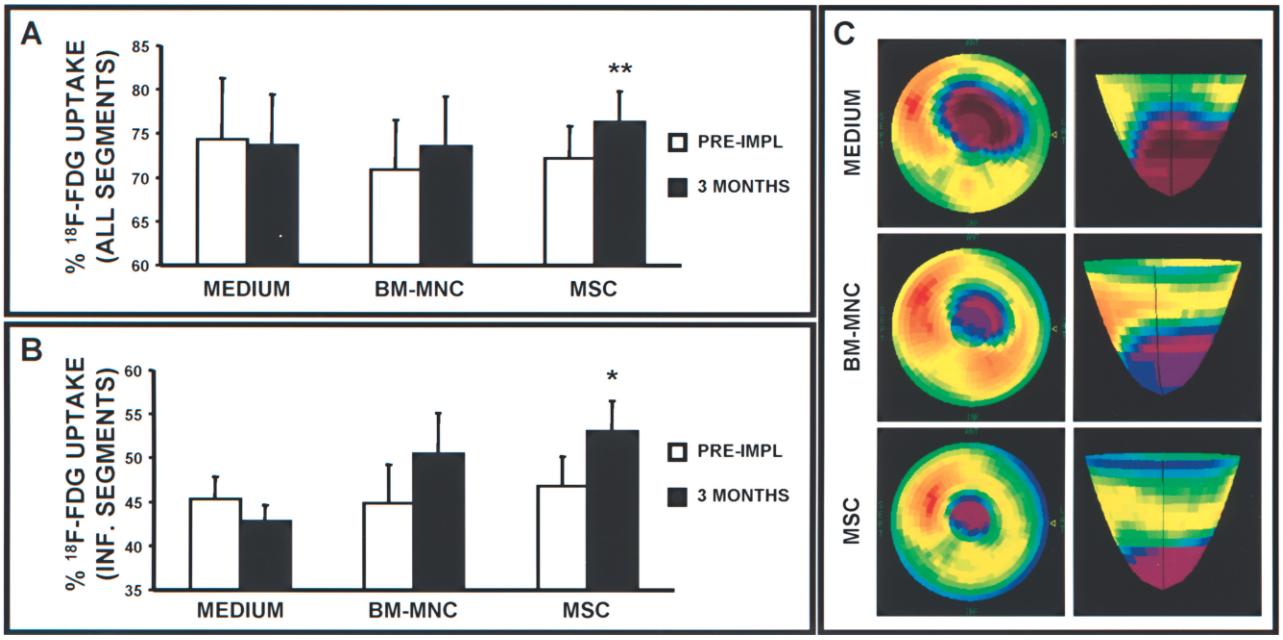

Figure 3. MSC positively affect tissue metabolism. ^{18}F-FDG uptake was evaluated by microPET before and 3 months after transplantation. A significant increase in the tissue metabolism was detected in the MSC-treated but not in the BM-MNC-treated hearts when all 17 segments were analyzed (mean ± SD, **$p < 0.01$) (A) and also when only the infarcted ones were analyzed (*$p < 0.05$) (B). Representative images (cross and longitudinal views) of the hearts, 3 months after cell or medium injection, are shown (C).

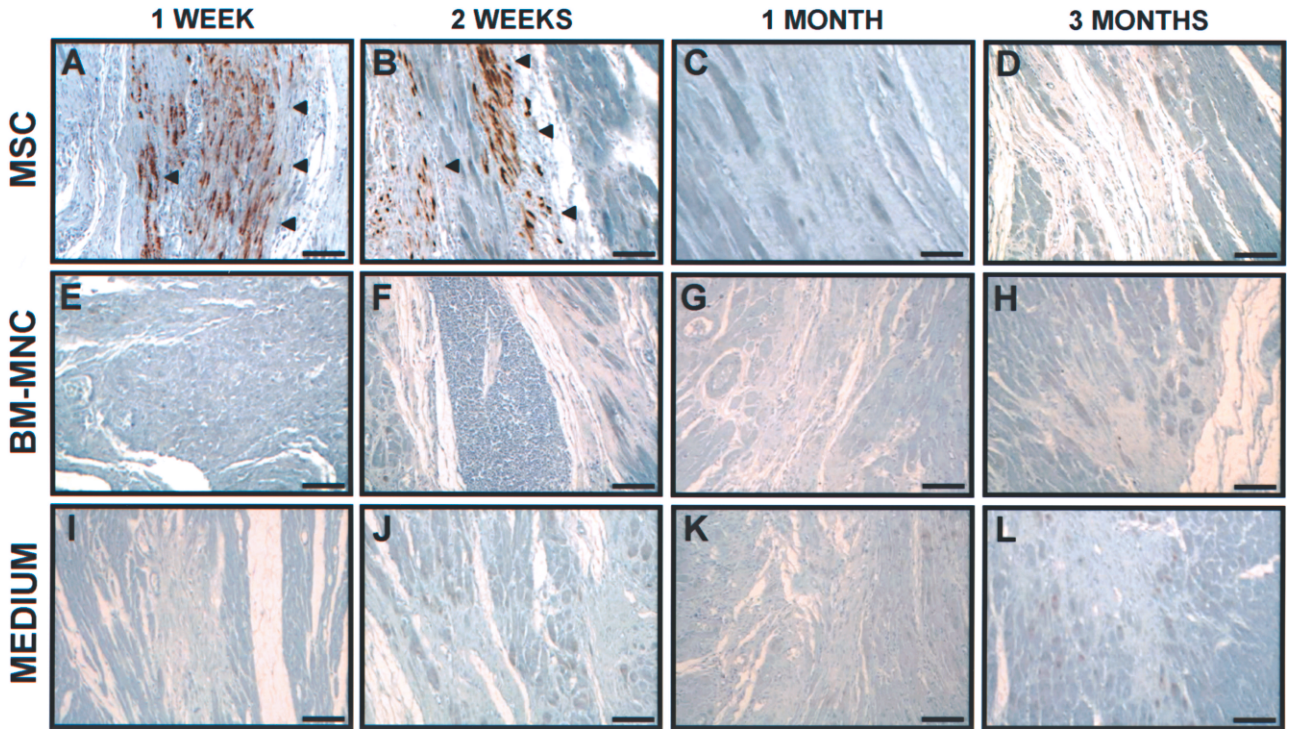

Figure 4. Cell engraftment. Presence of transplanted cells was assessed by immunohistochemistry against GFP at 1 and 2 weeks and 1 and 3 months after their injection. Engraftment was only detected for MSC at 1 and 2 weeks. (A–D) DMEM; (E–H) BM-MNC; (I–L) MSC. Scale bars: 100 μm.

167.48 ± 39.91 positive cells/mm^2). MSC-transplanted animals did also show an increase in CD68-positive cells, albeit significantly lower than BM-MNC (intra-infarct: 230.86 ± 59.27 positive cells/mm^2, $p < 0.01$ vs. medium; peri-infarct: 427.21 ± 71.7 positive cells/mm^2; $p < 0.01$ vs. control; $p < 0.01$ vs. BM-MNC). The increase in macrophage infiltration in the BM-MNC-transplanted animals was not due to the direct contribution of the transplanted cells as demonstrated by the lack of CD68$^+$/GFP$^+$ cells. Furthermore, double staining for GFP and CD68 revealed a strong infiltration of macrophages in close contact with injected MSC (Fig. 5I–M). Presence of GFP vesicles could be detected in the inflammatory cells by immunofluorescence (Fig. 5M) and confirmed by electronic microscopy (Fig. 6), suggesting host cell-mediated immune rejection of the transplanted cells.

MSC Do Not Differentiate Towards Vascular or Cardiac Phenotypes In Vivo

In vivo differentiation of MSC was analyzed by double immunofluorescence with antibodies against GFP and lineage-specific markers in tissue obtained at 1 and 2 weeks posttransplant. Transplanted MSC did not colocalize with endothelial markers such as caveolin-1, indicating lack of differentiation to endothelium (data not shown). On the other hand, although α-SMA-GFP cells were detected [percentage of double positive cells: 1 week: 12.80 (7.5; 20.6); 2 weeks 9.48 (10; 20.74), median (Q25; Q75)], these cells did not form vessel-like structures remaining with a fibroblastic morphology consistent with myofibroblast (Fig. 7A). Furthermore, expression of this marker was not surprising, as MSC do express α-SMA in in vitro culture (data not shown). Cardiac contribution could not be detected by double staining for GFP and the cardiac markers MLC2v or cTT (data not shown).

In order to confirm these data and identify the phenotypic identity of the mesenchymal cells once transplanted, electron microscopy after preembedding immunohistochemistry for GFP was performed. Four rats sacrificed 1 or 2 weeks after injection were studied and a mean of 30 cells/rat were analyzed. Confirming the results obtained in the immunofluorescence analysis, no vascular or cardiac GFP-positive cells were found and GFP-positive cells showed a typical fibroblastic phenotype with an elongated nucleus with a central nucleolus, small clumps chromatin organization, and a high density of RER cisterns (Fig. 7B). Implanted cells also presented big dictosomes and large mitochondrias and caveoli (Fig. 7B, arrowheads) along their surface. Interestingly, a consistent collagen network was found around them (Fig. 7B, asterisks).

On the other hand, although vascular or cardiac direct

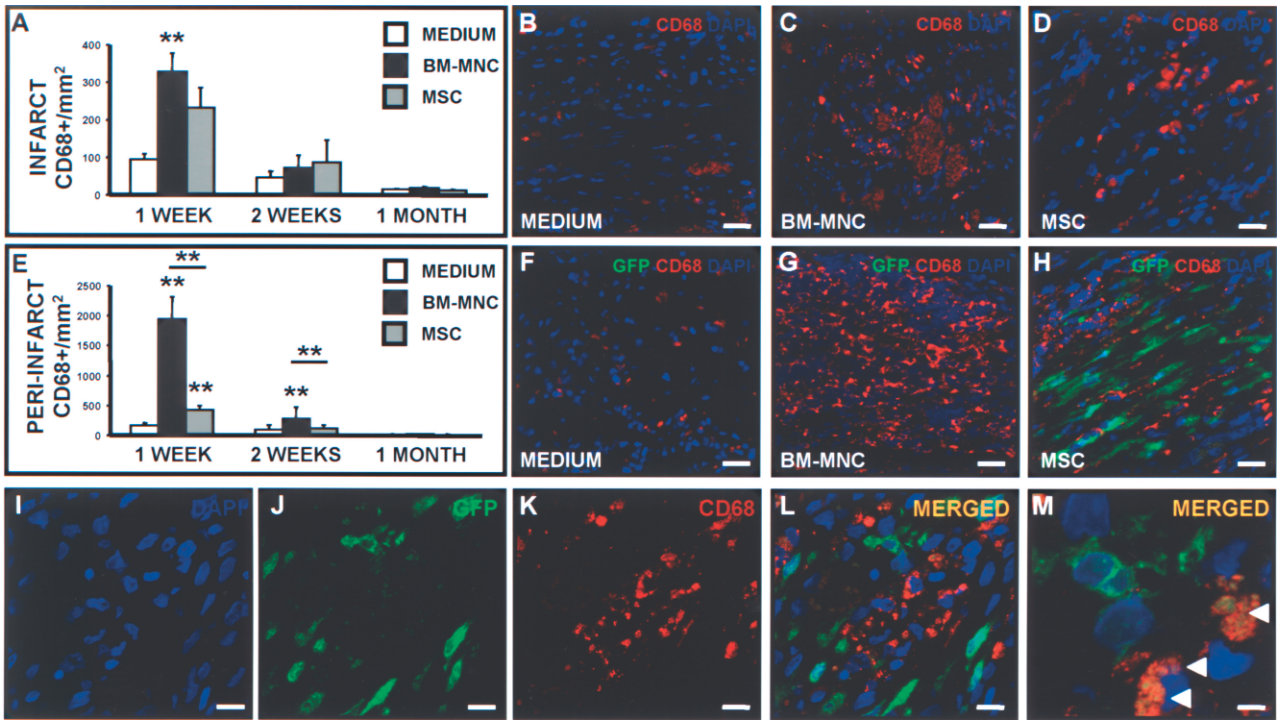

Figure 5. Cell transplantation in chronic MI is associated with macrophage infiltration. Sections of hearts obtained 1 and 2 weeks and 1 and 3 months after cell or media transplant were stained with antibodies against CD68 (red) and GFP (green) and macrophage infiltration was quantified as described in Materials and Methods. A significant (**$p < 0.01$) increase in macrophage density within the infarcted area of BM-MNC-implanted but not of MSC-implanted animals was found (A–D). Also in the peri-infarct area, there was a significant increase (**$p < 0.01$) in CD68-positive cell density in the peri-infarct region of BM-MNC- and MSC-treated rats, although this was less pronounced in the MSC than in the BM-MNC group (**$p < 0.01$) (E–H). Detailed CD68-positive macrophages infiltrating MSC injection areas are shown (I–M) with detectable GFP-positive vesicles in some of the phagocytes (arrowheads) (M). Images correspond to animals sacrificed 1 week after cell or medium injection. CD68 marker (Alexa-594): red; GFP (Alexa-488): green; nuclear staining (TOPRO3): blue. Scale bars: (B–D, F–H) 35 μm; (I–L) 20 μm; (M) 5 μm.

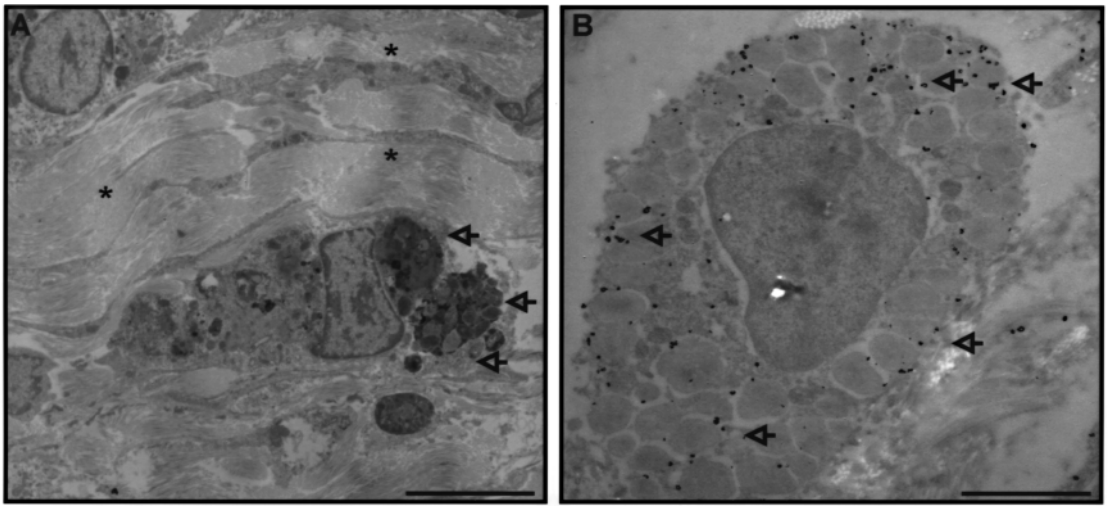

Figure 6. Electron microscopy of macrophages within cell-engrafted areas. One week after MSC transplantation, presence of macrophages (arrowheads) was confirmed by electronic microscopy, in the areas of cell injection (collagen deposits are indicated with asterisks) (A). A higher magnification field shows a GFP vesicle-containing macrophage. GFP deposits could be detected after previous immunogold GFP staining (arrowheads) (B). Scale bars: (A) 6 μm; (B) 2 μm.

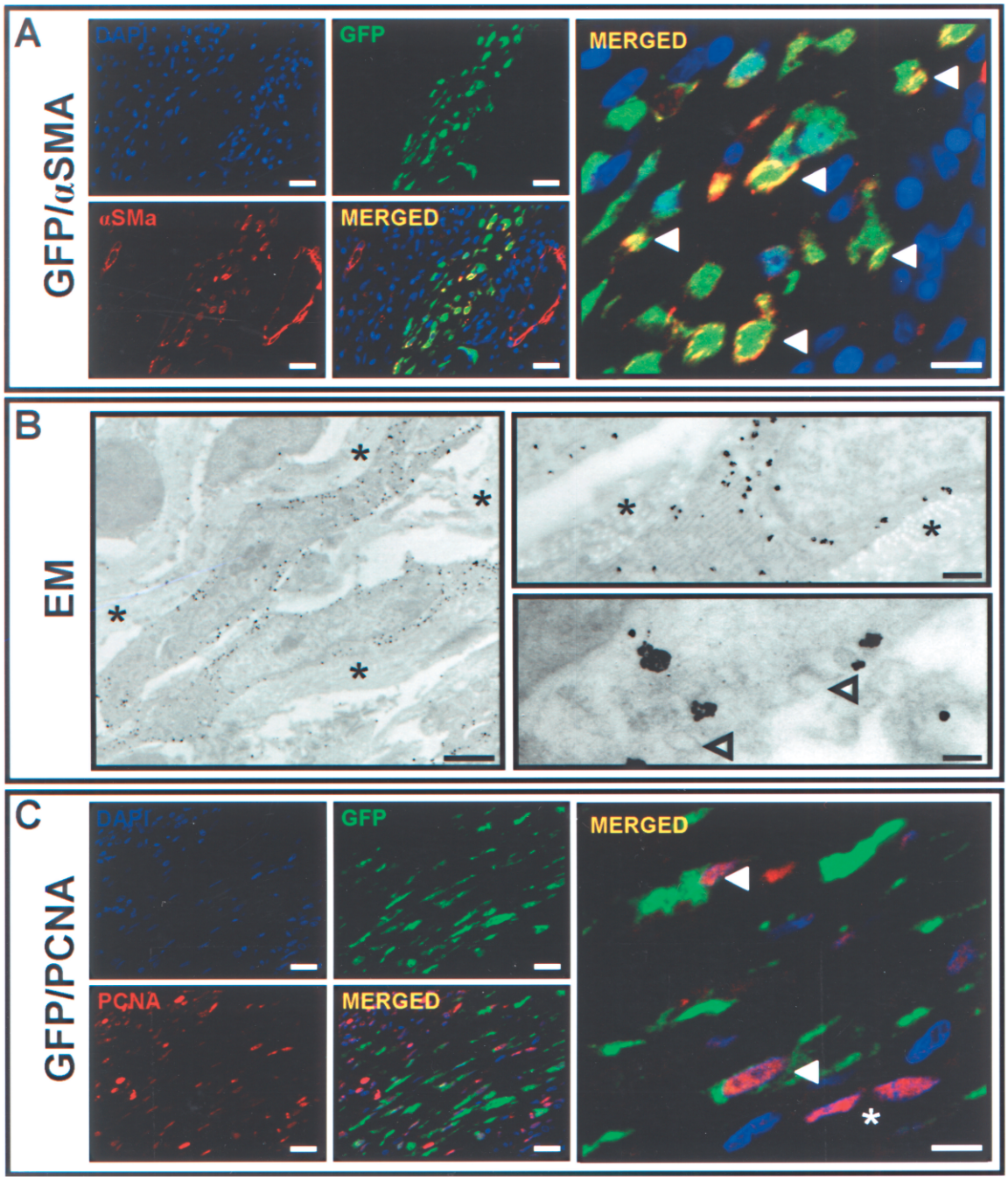

Figure 7. Analysis of cell fate and in vivo proliferation. One and 2 weeks after transplant, heart sections were stained with antibodies against α-SM-actin-Cy3 and PCNA (Alexa-594: red) and GFP (Alexa-488: green). Nuclear staining was performed with TOPRO3 (blue). Expression of lineage-specific markers was tested by double immunofluorescence. Engrafted GFP-MSC were positive for α-SM-actin (higher magnification field: arrowheads) although remained as myofibroblasts and did not contribute to the vascular net (A). Proliferating GFP-positive MSC (arrowheads) were also observed surrounded by proliferating non-GFP cells (asterisks) (B). GFP-positive cells were identified after GFP immunogold staining as fibroblast-like cells, which were surrounded by areas of collagen deposition (asterisks). Top right: higher magnification showing a GFP-positive cell; bottom right: caveoli in the membrane of GFP-MSC (arrowheads) (C). Images were taken from animals sacrificed 1 week after treatment. Scale bars: (A, B) 25 μm; higher magnification (B): 10 μm; (C) 2 μm; top right: 400 nm; bottom right: 100 nm.

contribution could not be detected, a small percentage of engrafted MSC (approximately 10% of engrafted cells at 1 week) did costained with PCNA (Fig. 7C, arrowheads), indicating their ability to proliferate within the damaged tissue. GFP cycling cells were not detected after 2 weeks posttransplant, suggesting either that proliferation occurred during a short time or that immune rejection was involved in the lack of proliferating cells. Interestingly, non-GFP cells located in the area of injection also expressed PCNA (Fig. 7C, asterisks), suggesting an (auto)paracrine effect of the MSC that promotes cell proliferation. Although most proliferating cells were of hematopoietic lineage (not shown), cell-implanted animals also showed a marked increase in the density of endothelial-proliferating cells both in the peri-infarct and infarct regions in the groups of animals treated with MSC (peri-infarct: 1 week: 69.44 ± 13 cells/mm^2; 2 weeks: 56.88 ± 5.29 cells/mm^2; $p < 0.01$ vs. medium; infarct: 1 week: 100 ± 16.61 cells/mm,sup>2; 2 weeks: 48.73 ± 14.13 cells/mm^2; $p < 0.01$ vs. medium) and BM-MNC (peri-infarct: 78.19 ± 11.26 cells/mm^2; 2 weeks: 54.13 ± 10.99 cells/mm^2; $p < 0.01$ vs. medium; infarct: 1 week: 42.89 ± 8.5 cells/mm^2; 2 weeks: 38.27 ± 7.97 cells/mm^2; $p < 0.01$ vs. medium) (Fig. 8A). MSC-treated hearts also presented an augmented density of cycling myofibroblasts (peri-infarct: 1 week: 113.17 ± 26.57 cells/mm^2; 2 weeks: 43.57 ± 10.03 cells/mm^2; $p < 0.01$ vs. medium; $p < 0.01$ vs. BM-MNC) that were rarely found in BM-MNC-treated animals and even less in control animals. Finally, although some dividing smooth muscle cells were identified, their numbers were only significantly increased in MSC-treated animals 1 week after injection (17.49 ± 6.08 cells/mm^2; $p < 0.05$ vs. medium). Representative images are shown in Figure 8B. No proliferating endothelial cells, myofibroblasts, or smooth muscle cells were detected 1 or 2 weeks after media injection (6 and 7 weeks after myocardial infarction) in animals treated with media alone.

MSC Promotes Revascularization and Cardiac Remodeling

Despite the low engraftment rate and the lack of differentiation, a functional benefit was detected in the rats transplanted with bone marrow-derived cells, with a stronger benefit in the animals treated with MSC. In order to elucidate the mechanisms involved in such functional improvement, we analyzed the effect of treatment on angiogenesis and vasculogenesis. Capillary density was determined 3 months after injection, by quantifying the small-caliber caveolin-1-positive vessels/mm^2 present in the peri-infarct region. As depicted in Figure 9A, only transplantation of MSC was able to induce a significant increase in vessel count (medium: 683.9 ± 37.8 capillaries/mm^2; BM-MNC: 705.8 ± 38.8 capillaries/mm^2; MSC: 897.1 ± 61.6 capillaries/mm^2; $p < 0.05$) (Fig. 9B–D). On the other hand, both cell treatments induced an increase in big caliber vessels, quantified as α-SMA-positive vessels/mm^2 (medium: 64.1 ± 5.4; BM-MNC: 130.1 ± 11; MSC: 145.7 ± 7.8; $p < 0.01$ in both cell-treated groups vs. medium) and α-SMA-positive area (medium: $1.2 \pm 0.1\%$; BM-MNC: $2.09 \pm 0.14\%$; MSC: $2.53 \pm 0.15\%$; $p < 0.01$ in both cell-treated groups vs. medium). Importantly, such increase in arterioles/arteries density in the peri-infarct region was significantly higher in the animals treated with MSC than in the BM-MNC-treated animals ($p < 0.01$ MSC vs. BM-MNC) (Fig. 9E–H).

As together with the revascularization processes, tissue remodeling may have an important role in the functional benefits. We analyzed infarct size and collagen content in the treated versus control animals and, as shown in Figure 9I–L, MSC- but not BM-MNC-treated hearts induced a significant decrease in infarct size compared to medium-injected controls (medium: $19.66 \pm 1.21\%$; BM-MNC: $17.47 \pm 4.62\%$; MSC: $12.78 \pm 1.66\%$; $p < 0.05$, percentages referred to the total LV area). Furthermore, a smaller infarct was associated with a decrease in collagen vascular fraction (CVF) (Fig. 9M–P) in MSC-injected animals (control group: $66.26 \pm 0.93\%$; BM-MN: $63.77 \pm 8.53\%$; MSC: $58.54 \pm 1.36\%$, $p < 0$ 05), showing a positive correlation between both parameters ($R^2 = 0.73$, $p < 0.01$), thereby demonstrating the superior effect of the MSC versus the BM-MNC.

DISCUSSION

In this study, the rigorous comparison of the long-term effect of two bone marrow derived populations, BM-MNC and MSC, in a chronic model of myocardial infarction indicates that transplantation of both BM stem cell populations induced a similar functional improvement but, importantly, that MSC induced a greater effect in the injured hearts that resulted in a smaller infarct size and scar collagen content with an increase in revascularization of the tissue. These effects eventually correlated with an increased tissue metabolism and a functional improvement in the contractile capacity of the myocardium.

Different factors might be responsible for the superior effect of the MSC over the BM-MNC, including a direct cell contribution to the vascular or cardiac tissue and/or a positive trophic effect. In accordance with previous studies with different populations of stem cells in which the limited cell engraftment supports a paracrine effect as the responsible for the functional benefit (27–29), neither BM-MNC nor MSC could be detected after 2 weeks posttransplantation, which discards a long-term direct contribution of engrafted cells to the tissue. In the case of the MSC, cells were detected for up to 2 weeks

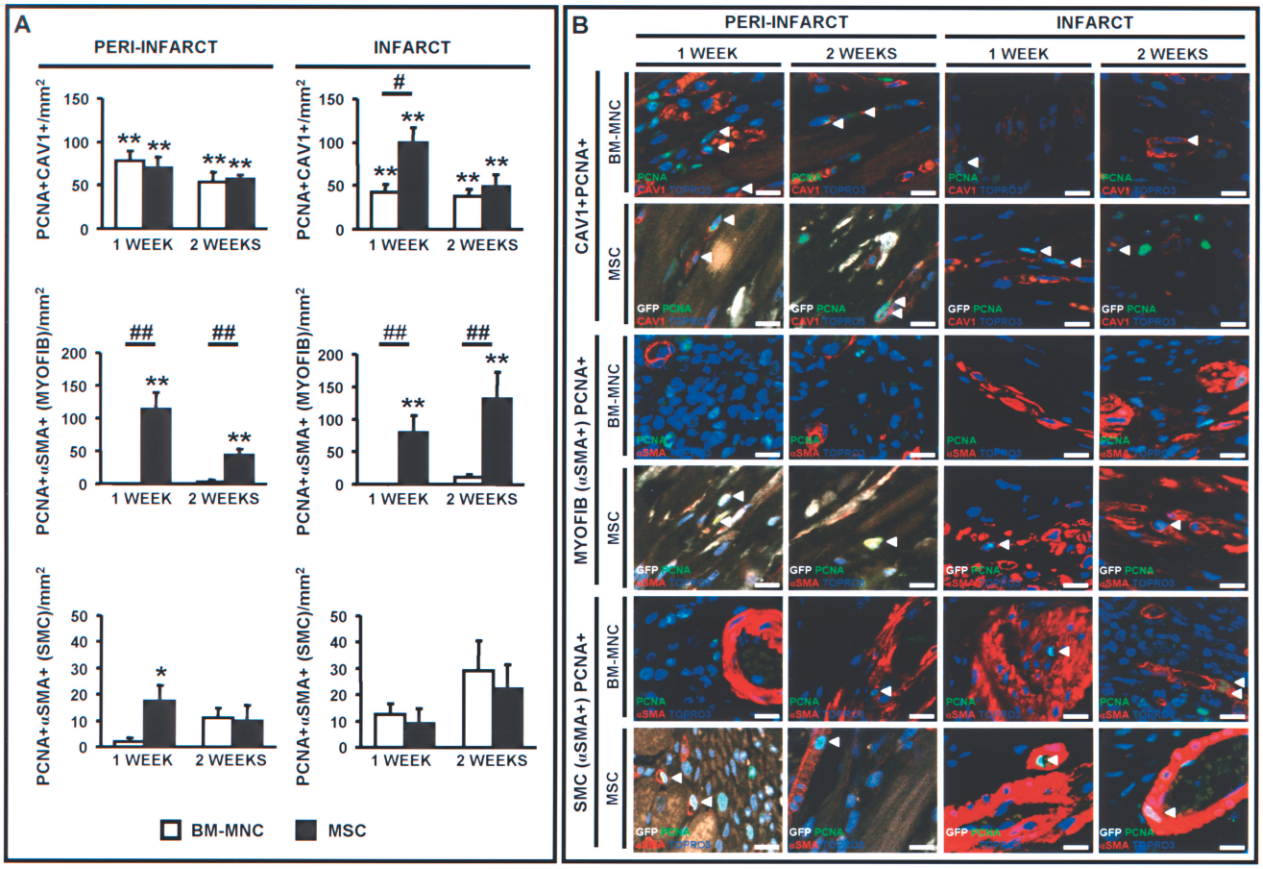

Figure 8. Host cell proliferation. Percentage of proliferating endothelial cells (caveolin-1 positive), myofibroblasts (α-SMA positive, spindle shape), or smooth muscle cells (α-SMA positive, forming vessels) was determined by quantification of PCNA-positive cells, within the peri-infarct and infarct areas 1 and 2 weeks after treatment (*$p < 0.05$ vs. medium-injected animals; **$p < 0.01$ vs. medium-treated rats; #$p < 0.05$ BM-MNC vs. MSC: ##$p < 0.01$ BM-MNC vs. MSC) (A). Representative pictures of proliferating endothelial cells ($PCNA^+Cav1^+$), myofibroblasts ($PCNA^+\alpha\text{-}SMA^+$, spindle shape), and smooth muscle cells ($PCNA^+\alpha\text{-}SMA^+$, vessels) within the peri-infarct and the infarct areas at 1 and 2 weeks performed by confocal microscopy, are shown (arrowheads: PCNA-positive cells) (B). GFP (Quantum Dot-655): white; caveolin-1 (Alexa-594) and α-SMA-Cy3 markers: red; PCNA (Alexa-488): green; nuclear staining (TOPRO-3): blue. Scale bars: 15 μm.

but a direct contribution to the vascular or cardiac tissue was ruled out as no differentiated cells were found. Some other studies, but not all, have reported cardiovascular differentiation of MSC (6,58) but it is still not clear if the reported putative cardiac differentiation was due to fusion events (5). Thereby, our results support an indirect trophic induction, as previously reported (28,50) in several in vivo models of acute ischemia (10,15,20, 52,60,61,64) and wound healing (11).

Differences in the cytokines expressed by each cell population or even the longer period of time in which cells were detected in the heart might explain the differences observed between the effects of BM-MNC and MSC. Interestingly, a recent comparative study performed in a rodent acute model of MI (59) has shown a better functional income of BM-MNC- than MSC-treated animals. These apparently contradictory results could be explained by the differences in the protocol model such as cell dose (five times higher in the cited study), duration of follow-up (6 weeks vs. 3 months) and, most importantly, timing of cell transplantation. Several factors differentiate the acute versus the chronic stage, like inflammation, fibrosis, or tissue remodeling [reviewed in (14,23)] and could explain the differential effect of transplanted cells with a stronger inflammatory/angiogenic effect of transplanted mononuclear cells in the acute stage versus a more potent effect in the tissue remodeling of the mesenchymal cells at the chronic stage. Therefore, our results highlight the clinical implications for the selection of the cell type according to the underlying disease.

On the other hand, despite of the positive and promising long-term results obtained, the poor survival of the cells remains as the main limitation of the study. A harsh

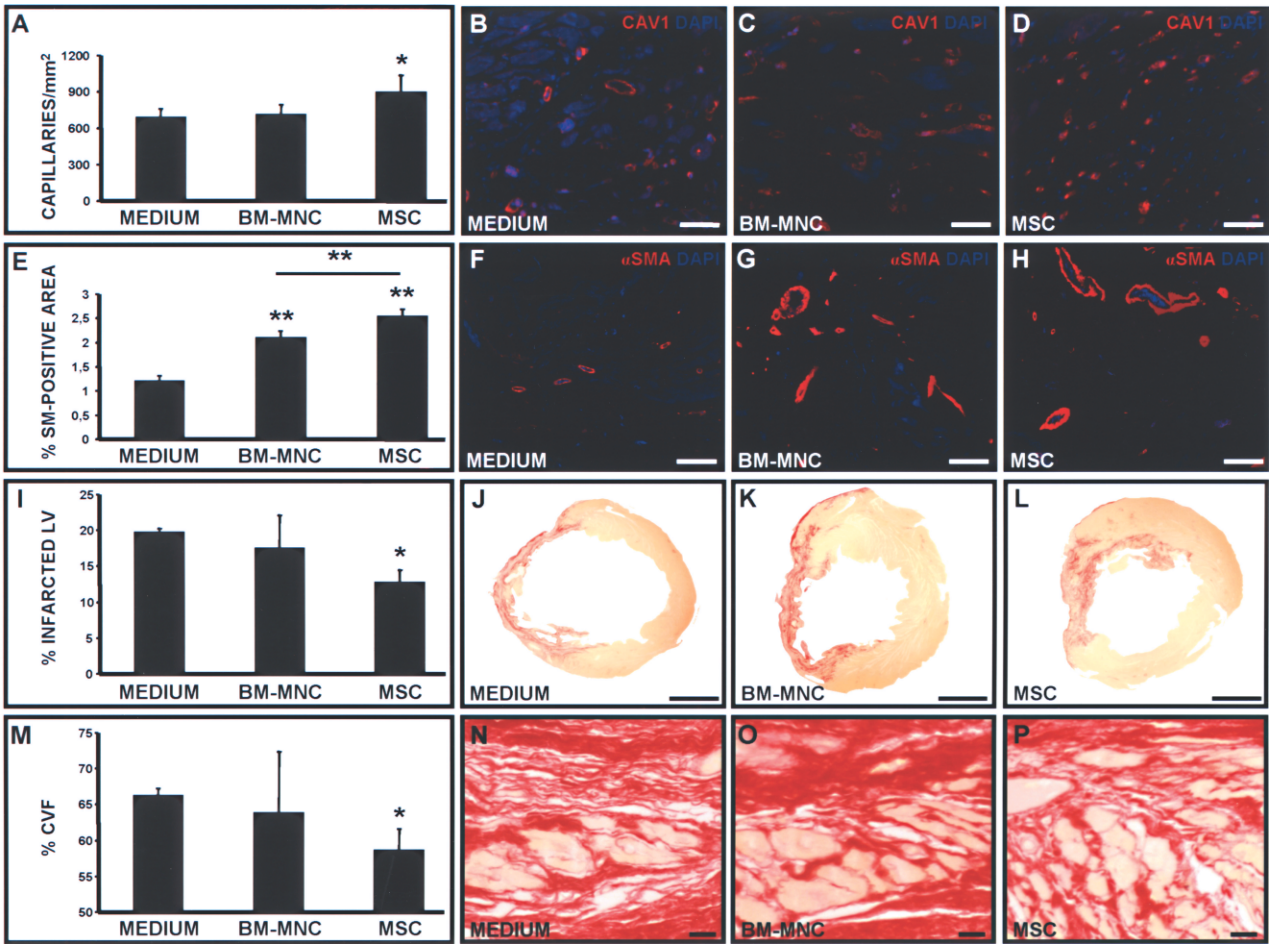

Figure 9. Cell transplant is associated with an increase in vasculogenesis/angiogenesis and decreased in fibrosis and infarct size. Capillary and arterioles/arteries densities were respectively determined by quantification of the small-caliber (5–10 μm) caveolin-1-positive capillaries/mm^2 (mean ± SD) (A–D) and α-SMA-positive area (%) (mean ± SD) (E–H) in the peri-infarcted zones, 3 months after media or cell (BM-MNC or MSC) transplant. A significant increase in capillary (*$p < 0.05$) (A) and in arterioles/arteries area (**$p < 0.01$) (E) was determined in the MSC-treated hearts (D, H) in comparison with the media-treated ones (B, F). On the contrary, BM-MNC did not exert any effect in the capillary density (C) and, albeit, it positively affected the big vessel revascularization (*$p < 0.05$) (G); this increase was significantly lower than in the MSC group (H) (**$p < 0.01$). Representative images of immunofluorescence for caveolin-1 (B–D) or α-SMA (F–H) staining are shown. Vessel markers (Alexa-594): red; nuclear staining (DAPI): blue. Morphometric analysis in serial sirius red-stained sections (I–P) showed also a significant smaller scar size (*$p < 0.05$) in the left ventricles of the MSC-treated hearts in comparison with the media-treated hearts, 3 months posttransplantation (I–L). Furthermore, fibrosis degree in the infarcted zone was also significantly smaller in the MSC group (*$p < 0.05$). BM-MNC did not have a positive effect either in the scar size or in the fibrosis degree (M–P). Scale bars: (B–D, F–H, N–P) 100 μm; (J–L) 2.5 mm.

scar tissue environment and the immunogenicity of the GFP are potential factors explaining the rapid cell disappearance. We have to consider that, in our model, immunosuppression with cyclosporin A inhibited T-cell-mediated response but not monocyte/macropages action, which can react against the GFP neoantigen as we have demonstrated in this study and consistent with previous reports (33). In the case of the BM-MNC, which elicited a remarkable inflammatory response, the effect could be faster than with the MSC, paying for the shorter presence of cells in the injured tissue. On top of the GFP response, the MNC bone marrow fraction may contain mature immune cells and precursors that could elicit a stronger immune response. On the other hand, MSC has been reported to exert an immunomodulatory effect, which could have delayed or blunted the process (31). Improvement of cell engraftment remains a major goal for cell therapy. In fact, several reports have shown a greater benefit when MSC were genetically modified by, for example, transfection of vectors that overexpressed

the Akt protein or the hypoxia-regulated heme oxygenase 1 (38,55) or when administered together with cytokine cocktails (i.e., IGF-1) (12,17) that favored their survival once transplanted. A different approach has used MSC grown in vitro over matrices that can be applied to the myocardium, thereby facilitating their engraftment (44). These strategies should be able to improve cell retention and survival or even promote the differentiation of the cells towards desired cell phenotypes.

Another interesting finding related to the potential mechanism of tissue repair after cell therapy was the induction of proliferation of host cells. It is conceivable that the release of growth factors such as VEGF, HGF, and bFGF could contribute to cell proliferation and cell survival, consistent with previous studies with MSC (2, 47,56), while the release of SDF1 (63) could stimulate BM progenitor cell homing (1). Our study supports the role of transplanted cells in the in vivo induction of proliferation of host cells such as endothelial and smooth muscle cells, as previously described in vitro (28,29). Despite cell proliferation being a short-term effect (we could only observed a significant proliferation for up to 2 weeks after transplant but not at 1 at 3 months), the effects were long term, as demonstrated by the increase in angiogenesis and vasculogenesis for up to 3 months posttransplantation. It is important to note that no cell proliferation was found in animals in which only media was administered, consistent which the fact that the acute MI was induced more that 7 weeks before, a period of time in which healing of the myocardium in rats has ensued. In addition, our results showing the induction of host-derived myofibroblast proliferation after injection of MSC, key players in the process of scar regeneration and maturation [reviewed in (54)] not only as main collagen-depositors, but also for their secretion of metalloproteinases, suggest that myofibroblast as well as the proinflammatory microenvironment provided by the $CD68^+$ cell infiltration could stimulate an antifibrotic phenotype of the cardiac fibroblasts (8).

A remarkable finding in our study was the very significant macrophage infiltration observed in both groups of cell-treated animals, which has not been frequently reported in other cell therapy studies (18). Macrophages were observed both in animals treated with MSC and BM-MNC but not in the media control animals, suggesting that transplanted cells were responsible for inducing such infiltrate, which was significantly greater in BM-MNC-treated animals and was not contributed by transplanted cells (no GFP-positive macrophages). Macrophage infiltration is associated with the normal healing process after MI. A recent report demonstrates that hearts modulate their chemokine expression profile over time after MI, recruiting different types of monocytes (46). During the initial phase monocytes exhibit phagocytic, proteolytic, and inflammatory functions, while during a later phase, monocytes promote healing via myofibroblast accumulation, angiogenesis, and deposition of collagen (46). The potential of monocytes/macrophages to contribute to healing of the myocardium has also been described in recent studies (7,11,18). Transplanted cells may in fact increase these processes by stimulating the recruitment of more inflammatory cells. Whether macrophage infiltration is due to the release of growth factors or to an immune-mediated rejection process as mentioned above cannot be ruled out, but in any case may contribute to the beneficial effect. The greater macrophage infiltrate observed after BM-MNC could also be responsible for the faster clearance of the cells and should be taken into account as most of the clinical trials performed with stem cells have been performed with bone marrow-derived mononuclear cells.

In summary, we conclude that transplantation of MSC provide a long-term beneficial effect in cardiac function and remodeling even when hearts are chronically injured, despite the lack of direct contribution of the transplanted cells. Furthermore, this is the first study where the potential of MSC and freshly isolated BM-MNC has been comparatively studied in a chronic model, showing that despite some positive effect in cardiac performance by BM-MNC, MSC had a clear superior effect. We believe that given the demonstrated potential of the MSC, it should be a population to consider for future clinical trials not only in the acute but also in the chronic setting of the disease.

ACKNOWLEDGMENTS: Grant support from Ministerio de Sanidad PI050168 and ISCIII-RETIC RD06/0014, Gobierno de Navarra (Departamento de Educación), Comunidad de Trabajo de los Pirineos (CTP), European Union Framework Project VII (INELPY), Caja de Ahorros de Navarra (Programa Tu Eliges: Tu Decides), and the 'UTE project CIMA" to F.P. and Ministerio de Sanidad PI070474 to B.P.

REFERENCES

1. Abbott, J. D.; Huang, Y.; Liu, D.; Hickey, R.; Krause, D. S.; Giordano, F. J. Stromal cell-derived factor-1alpha plays a critical role in stem cell recruitment to the heart after myocardial infarction but is not sufficient to induce homing in the absence of injury. Circulation 110:3300–3305; 2004.
2. Adamek, A.; Hu, K.; Bayer, B.; Wagner, H.; Ertl, G.; Bauersachs, J.; Frantz, S. High dose aspirin and left ventricular remodeling after myocardial infarction: Aspirin and myocardial infarction. Basic Res. Cardiol. 102:334–340; 2007.
3. Agbulut, O.; Mazo, M.; Bressolle, C.; Gutierrez, M.; Azarnoush, K.; Sabbah, L.; Niederlander, N.; Abizanda, G.; Andreu, E. J.; Pelacho, B.; Gavira, J. J.; Perez-Ilzarbe, M.; Peyrard, S.; Bruneval, P.; Samuel, J. L.; Soriano-Navarro, M.; Garcia-Verdugo, J. M.; Hagege, A. A.; Prosper, F.; Menasche, P. Can bone marrow-derived multipotent adult progenitor cells regenerate infarcted myocardium? Cardiovasc. Res. 72:175–183; 2006.

4. Aggarwal, S.; Pittenger, M. F. Human mesenchymal stem cells modulate allogeneic immune cell responses. Blood 105:1815–1822; 2005.
5. Alvarez-Dolado, M.; Pardal, R.; Garcia-Verdugo, J. M.; Fike, J. R.; Lee, H. O.; Pfeffer, K.; Lois, C.; Morrison, S. J.; Alvarez-Buylla, A. Fusion of bone-marrow-derived cells with Purkinje neurons, cardiomyocytes and hepatocytes. Nature 425:968–973; 2003.
6. Amado, L. C.; Saliaris, A. P.; Schuleri, K. H.; St John, M.; Xie, J. S.; Cattaneo, S.; Durand, D. J.; Fitton, T.; Kuang, J. Q.; Stewart, G.; Lehrke, S.; Baumgartner, W. W.; Martin, B. J.; Heldman, A. W.; Hare, J. M. Cardiac repair with intramyocardial injection of allogeneic mesenchymal stem cells after myocardial infarction. Proc. Natl. Acad. Sci. USA 102:11474–11479; 2005.
7. Armstrong, P. W.; Granger, C. B.; Adams, P. X.; Hamm, C.; Holmes, Jr., D.; O'Neill, W. W.; Todaro, T. G.; Vahanian, A.; Van de Werf, F. Pexelizumab for acute ST-elevation myocardial infarction in patients undergoing primary percutaneous coronary intervention: A randomized controlled trial. JAMA 297:43–51; 2007.
8. Brown, R. D.; Jones, G. M.; Laird, R. E.; Hudson, P.; Long, C. S. Cytokines regulate matrix metalloproteinases and migration in cardiac fibroblasts. Biochem. Biophys. Res. Commun. 362:200–205; 2007.
9. Bujak, M.; Frangogiannis, N. G. The role of TGF-beta signaling in myocardial infarction and cardiac remodeling. Cardiovasc. Res. 74:184–195; 2007.
10. Burchfield, J. S.; Iwasaki, M.; Koyanagi, M.; Urbich, C.; Rosenthal, N.; Zeiher, A. M.; Dimmeler, S. Interleukin-10 from transplanted bone marrow mononuclear cells contributes to cardiac protection after myocardial infarction. Circ. Res. 103:203–211; 2008.
11. Chen, L.; Tredget, E. E.; Wu, P. Y.; Wu, Y. Paracrine factors of mesenchymal stem cells recruit macrophages and endothelial lineage cells and enhance wound healing. PLoS ONE 3:e1886; 2008.
12. Davis, M. E.; Hsieh, P. C.; Takahashi, T.; Song, Q.; Zhang, S.; Kamm, R. D.; Grodzinsky, A. J.; Anversa, P.; Lee, R. T. Local myocardial insulin-like growth factor 1 (IGF-1) delivery with biotinylated peptide nanofibers improves cell therapy for myocardial infarction. Proc. Natl. Acad. Sci. USA 103:8155–8160; 2006.
13. D'Ippolito, G.; Diabira, S.; Howard, G. A.; Menei, P.; Roos, B. A.; Schiller, P. C. Marrow-isolated adult multilineage inducible (MIAMI) cells, a unique population of postnatal young and old human cells with extensive expansion and differentiation potential. J. Cell Sci. 117: 2971–2981; 2004.
14. Ertl, G.; Frantz, S. Healing after myocardial infarction. Cardiovasc. Res. 66:22–32; 2005.
15. Frantz, S.; Vallabhapurapu, D.; Tillmanns, J.; Brousos, N.; Wagner, H.; Henig, K.; Ertl, G.; Muller, A. M.; Bauersachs, J. Impact of different bone marrow cell preparations on left ventricular remodelling after experimental myocardial infarction. Eur. J. Heart Fail. 10:119–124; 2008.
16. Gavira, J. J.; Perez-Ilzarbe, M.; Abizanda, G.; Garcia-Rodriguez, A.; Orbe, J.; Paramo, J. A.; Belzunce, M.; Rabago, G.; Barba, J.; Herreros, J.; Panizo, A.; de Jalon, J. A.; Martinez-Caro, D.; Prosper, F. A comparison between percutaneous and surgical transplantation of autologous skeletal myoblasts in a swine model of chronic myocardial infarction. Cardiovasc. Res. 71:744–753; 2006.
17. Hahn, J. Y.; Cho, H. J.; Kang, H. J.; Kim, T. S.; Kim, M. H.; Chung, J. H.; Bae, J. W.; Oh, B. H.; Park, Y. B.; Kim, H. S. Pre-treatment of mesenchymal stem cells with a combination of growth factors enhances gap junction formation, cytoprotective effect on cardiomyocytes, and therapeutic efficacy for myocardial infarction. J. Am. Coll. Cardiol. 51:933–943; 2008.
18. Imanishi, Y.; Saito, A.; Komoda, H.; Kitagawa-Sakakida, S.; Miyagawa, S.; Kondoh, H.; Ichikawa, H.; Sawa, Y. Allogenic mesenchymal stem cell transplantation has a therapeutic effect in acute myocardial infarction in rats. J. Mol. Cell. Cardiol. 44:662–671; 2008.
19. Iop, L.; Chiavegato, A.; Callegari, A.; Bollini, S.; Piccoli, M.; Pozzobon, M.; Rossi, C. A.; Calamelli, S.; Chiavegato, D.; Gerosa, G.; De Coppi, P.; Sartore, S. Different cardiovascular potential of adult- and fetal-type mesenchymal stem cells in a rat model of heart cryoinjury. Cell Transplant. 17:679–694; 2008.
20. Iwase, T.; Nagaya, N.; Fujii, T.; Itoh, T.; Murakami, S.; Matsumoto, T.; Kangawa, K.; Kitamura, S. Comparison of angiogenic potency between mesenchymal stem cells and mononuclear cells in a rat model of hindlimb ischemia. Cardiovasc. Res. 66:543–551; 2005.
21. Janssens, S.; Dubois, C.; Bogaert, J.; Theunissen, K.; Deroose, C.; Desmet, W.; Kalantzi, M.; Herbots, L.; Sinnaeve, P.; Dens, J.; Maertens, J.; Rademakers, F.; Dymarkowski, S.; Gheysens, O.; Van Cleemput, J.; Bormans, G.; Nuyts, J.; Belmans, A.; Mortelmans, L.; Boogaerts, M.; Van de Werf, F. Autologous bone marrow-derived stem-cell transfer in patients with ST-segment elevation myocardial infarction: Double-blind, randomised controlled trial. Lancet 367:113–121; 2006.
22. Jawad, H.; Ali, N. N.; Lyon, A. R.; Chen, Q. Z.; Harding, S. E.; Boccaccini, A. R. Myocardial tissue engineering: A review. J. Tissue Eng. Regen. Med. 1:327–342; 2007.
23. Jennings, R. B.; Murry, C. E.; Steenbergen, Jr., C.; Reimer, K. A. Development of cell injury in sustained acute ischemia. Circulation 82:II2–12; 1990.
24. Jiang, Y.; Vaessen, B.; Lenvik, T.; Blackstad, M.; Reyes, M.; Verfaillie, C. M. Multipotent progenitor cells can be isolated from postnatal murine bone marrow, muscle, and brain. Exp. Hematol. 30:896–904; 2002.
25. Kalidindi, S. R.; Tang, W. H.; Francis, G. S. Drug insight: Aldosterone-receptor antagonists in heart failure—the journey continues. Nat. Clin. Pract. Cardiovasc. Med. 4: 368–378; 2007.
26. Keidar, S.; Kaplan, M.; Gamliel-Lazarovich, A. ACE2 of the heart: From angiotensin I to angiotensin (1–7). Cardiovasc. Res. 73:463–469; 2007.
27. Kinnaird, T.; Stabile, E.; Burnett, M. S.; Epstein, S. E. Bone-marrow-derived cells for enhancing collateral development: Mechanisms, animal data, and initial clinical experiences. Circ. Res. 95:354–363; 2004.
28. Kinnaird, T.; Stabile, E.; Burnett, M. S.; Lee, C. W.; Barr, S.; Fuchs, S.; Epstein, S. E. Marrow-derived stromal cells express genes encoding a broad spectrum of arteriogenic cytokines and promote in vitro and in vivo arteriogenesis through paracrine mechanisms. Circ. Res. 94:678–685; 2004.
29. Kinnaird, T.; Stabile, E.; Burnett, M. S.; Shou, M.; Lee, C. W.; Barr, S.; Fuchs, S.; Epstein, S. E. Local delivery of marrow-derived stromal cells augments collateral perfusion through paracrine mechanisms. Circulation 109: 1543–1549; 2004.
30. Kucia, M.; Reca, R.; Campbell, F. R.; Zuba-Surma, E.; Majka, M.; Ratajczak, J.; Ratajczak, M. Z. A population

of very small embryonic-like (VSEL) CXCR4(+)SSEA-1(+)Oct-4+ stem cells identified in adult bone marrow. Leukemia 20:857–869; 2006.
31. Le Blanc, K. Mesenchymal stromal cells: Tissue repair and immune modulation. Cytotherapy 8:559–561; 2006.
32. Levesque, J. P.; Winkler, I. G.; Larsen, S. R.; Rasko, J. E. Mobilization of bone marrow-derived progenitors. Handb. Exp. Pharmacol. 180:3–36; 2007.
33. Lin, Y.; Vandeputte, M.; Waer, M. Natural killer cell- and macrophage-mediated rejection of concordant xenografts in the absence of T and B cell responses. J. Immunol. 158: 5658–5667; 1997.
34. Lindsey, M. L. MMP induction and inhibition in myocardial infarction. Heart Fail. Rev. 9:7–19; 2004.
35. Lipinski, M. J.; Biondi-Zoccai, G. G.; Abbate, A.; Khianey, R.; Sheiban, I.; Bartunek, J.; Vanderheyden, M.; Kim, H. S.; Kang, H. J.; Strauer, B. E.; Vetrovec, G. W. Impact of intracoronary cell therapy on left ventricular function in the setting of acute myocardial infarction: A collaborative systematic review and meta-analysis of controlled clinical trials. J. Am. Coll. Cardiol. 50:1761–1767; 2007.
36. Liu, J. W.; Dunoyer-Geindre, S.; Serre-Beinier, V.; Mai, G.; Lambert, J. F.; Fish, R. J.; Pernod, G.; Buehler, L.; Bounameaux, H.; Kruithof, E. K. Characterization of endothelial-like cells derived from human mesenchymal stem cells. J. Thromb. Haemost. 5:826–834; 2007.
37. Lunde, K.; Solheim, S.; Aakhus, S.; Arnesen, H.; Abdelnoor, M.; Egeland, T.; Endresen, K.; Ilebekk, A.; Mangschau, A.; Fjeld, J. G.; Smith, H. J.; Taraldsrud, E.; Grogaard, H. K.; Bjornerheim, R.; Brekke, M.; Muller, C.; Hopp, E.; Ragnarsson, A.; Brinchmann, J. E.; Forfang, K. Intracoronary injection of mononuclear bone marrow cells in acute myocardial infarction. N. Engl. J. Med. 355: 1199–1209; 2006.
38. Mangi, A. A.; Noiseux, N.; Kong, D.; He, H.; Rezvani, M.; Ingwall, J. S.; Dzau, V. J. Mesenchymal stem cells modified with Akt prevent remodeling and restore performance of infarcted hearts. Nat. Med. 9:1195–1201; 2003.
39. Mann, D. L. Targeted anticytokine therapy and the failing heart. Am. J. Cardiol. 95:9C–16C; discussion 38C–40C; 2005.
40. McMurray, J. J.; Pfeffer, M. A. Heart failure. Lancet 365: 1877–1889; 2005.
41. Meller, J.; Herman, M. V.; Teichholz, L. E. Noninvasive assessment of left ventricular function. Adv. Intern. Med. 24:331–357; 1979.
42. Menasche, P.; Alfieri, O.; Janssens, S.; McKenna, W.; Reichenspurner, H.; Trinquart, L.; Vilquin, J. T.; Marolleau, J. P.; Seymour, B.; Larghero, J.; Lake, S.; Chatellier, G.; Solomon, S.; Desnos, M.; Hagege, A. A. The Myoblast Autologous Grafting in Ischemic Cardiomyopathy (MAGIC) trial: First randomized placebo-controlled study of myoblast transplantation. Circulation 117:1189–1200; 2008.
43. Meyer, G. P.; Wollert, K. C.; Lotz, J.; Steffens, J.; Lippolt, P.; Fichtner, S.; Hecker, H.; Schaefer, A.; Arseniev, L.; Hertenstein, B.; Ganser, A.; Drexler, H. Intracoronary bone marrow cell transfer after myocardial infarction: Eighteen months' follow-up data from the randomized, controlled BOOST (BOne marrOw transfer to enhance ST-elevation infarct regeneration) trial. Circulation 113: 1287–1294; 2006.
44. Miyahara, Y.; Nagaya, N.; Kataoka, M.; Yanagawa, B.; Tanaka, K.; Hao, H.; Ishino, K.; Ishida, H.; Shimizu, T.; Kangawa, K.; Sano, S.; Okano, T.; Kitamura, S.; Mori, H. Monolayered mesenchymal stem cells repair scarred myocardium after myocardial infarction. Nat. Med. 12: 459–465; 2006.
45. Murry, C. E.; Field, L. J.; Menasche, P. Cell-based cardiac repair: Reflections at the 10-year point. Circulation 112: 3174–3183; 2005.
46. Nahrendorf, M.; Swirski, F. K.; Aikawa, E.; Stangenberg, L.; Wurdinger, T.; Figueiredo, J. L.; Libby, P.; Weissleder, R.; Pittet, M. J. The healing myocardium sequentially mobilizes two monocyte subsets with divergent and complementary functions. J. Exp. Med. 204:3037–3047; 2007.
47. Ohnishi, S.; Yasuda, T.; Kitamura, S.; Nagaya, N. Effect of hypoxia on gene expression of bone marrow-derived mesenchymal stem cells and mononuclear cells. Stem Cells 25:1166–1177; 2007.
48. Pelacho, B.; Nakamura, Y.; Zhang, J.; Ross, J.; Heremans, Y.; Nelson-Holte, M.; Lemke, B.; Hagenbrock, J.; Jiang, Y.; Prosper, F.; Luttun, A.; Verfaillie, C. M. Multipotent adult progenitor cell transplantation increases vascularity and improves left ventricular function after myocardial infarction. J. Tissue Eng. Regen. Med. 1:51–59; 2007.
49. Penuelas, I.; Abizanda, G.; Garcia-Velloso, M. J.; Gavira, J. J.; Marti-Climent, J. M.; Ecay, M.; Collantes, M.; Garcia de Jalon, J. A.; Garcia-Rodriguez, A.; Mazo, M.; Barba, J.; Richter, J. A.; Prosper, F. 18F-FDG metabolism in a rat model of chronic infarction: A 17-sector semiquantitative analysis. Nuklearmedizin 46:149–154; 2007.
50. Perez-Ilzarbe, M.; Agbulut, O.; Pelacho, B.; Ciorba, C.; San Jose-Eneriz, E.; Desnos, M.; Hagege, A. A.; Aranda, P.; Andreu, E. J.; Menasche, P.; Prosper, F. Characterization of the paracrine effects of human skeletal myoblasts transplanted in infarcted myocardium. Eur. J. Heart Fail. 10:1065–1072; 2008.
51. Ramos, G. A.; Hare, J. M. Cardiac cell-based therapy: Cell types and mechanisms of actions. Cell Transplant. 16:951–961; 2007.
52. Schenke-Layland, K.; Strem, B. M.; Jordan, M. C.; Deemedio, M. T.; Hedrick, M. H.; Roos, K. P.; Fraser, J. K.; Maclellan, W. R. Adipose tissue-derived cells improve cardiac function following myocardial infarction. J. Surg. Res. 153(2):217–223; 2008.
53. Segers, V. F.; Lee, R. T. Stem-cell therapy for cardiac disease. Nature 451:937–942; 2008.
54. Sun, Y.; Kiani, M. F.; Postlethwaite, A. E.; Weber, K. T. Infarct scar as living tissue. Basic Res. Cardiol. 97:343–347; 2002.
55. Tang, Y. L.; Tang, Y.; Zhang, Y. C.; Qian, K.; Shen, L.; Phillips, M. I. Improved graft mesenchymal stem cell survival in ischemic heart with a hypoxia-regulated heme oxygenase-1 vector. J. Am. Coll. Cardiol. 46:1339–1350; 2005.
56. Tang, Y. L.; Zhao, Q.; Zhang, Y. C.; Cheng, L.; Liu, M.; Shi, J.; Yang, Y. Z.; Pan, C.; Ge, J.; Phillips, M. I. Autologous mesenchymal stem cell transplantation induce VEGF and neovascularization in ischemic myocardium. Regul. Pept. 117:3–10; 2004.
57. Tiyyagura, S. R.; Pinney, S. P. Left ventricular remodeling after myocardial infarction: Past, present, and future. Mt. Sinai J. Med. 73:840–851; 2006.
58. Toma, C.; Pittenger, M. F.; Cahill, K. S.; Byrne, B. J.; Kessler, P. D. Human mesenchymal stem cells differentiate to a cardiomyocyte phenotype in the adult murine heart. Circulation 105:93–98; 2002.

59. van der Bogt, K. E.; Sheikh, A. Y.; Schrepfer, S.; Hoyt, G.; Cao, F.; Ransohoff, K. J.; Swijnenburg, R. J.; Pearl, J.; Lee, A.; Fischbein, M.; Contag, C. H.; Robbins, R. C.; Wu, J. C. Comparison of different adult stem cell types for treatment of myocardial ischemia. Circulation 118: S121–129; 2008.
60. Xu, M.; Uemura, R.; Dai, Y.; Wang, Y.; Pasha, Z.; Ashraf, M. In vitro and in vivo effects of bone marrow stem cells on cardiac structure and function. J. Mol. Cell Cardiol. 42:441–448; 2007.
61. Yokokura, Y.; Hayashida, N.; Okazaki, T.; Nakamura, E.; Tayama, E.; Akashi, H.; Aoyagi, S. Influence of angiogenesis by implantation of bone marrow mononuclear cells in the rat ischemic heart. Kurume Med. J. 54:77–84; 2007.
62. Yoshimura, K.; Shigeura, T.; Matsumoto, D.; Sato, T.; Takaki, Y.; Aiba-Kojima, E.; Sato, K.; Inoue, K.; Nagase, T.; Koshima, I.; Gonda, K. Characterization of freshly isolated and cultured cells derived from the fatty and fluid portions of liposuction aspirates. J. Cell. Physiol. 208:64–76; 2006.
63. Zhang, M.; Mal, N.; Kiedrowski, M.; Chacko, M.; Askari, A. T.; Popovic, Z. B.; Koc, O. N.; Penn, M. S. SDF-1 expression by mesenchymal stem cells results in trophic support of cardiac myocytes after myocardial infarction. FASEB J. 21:3197–3207; 2007.
64. Zhang, S.; Ge, J.; Sun, A.; Xu, D.; Qian, J.; Lin, J.; Zhao, Y.; Hu, H.; Li, Y.; Wang, K.; Zou, Y. Comparison of various kinds of bone marrow stem cells for the repair of infarcted myocardium: Single clonally purified non-hematopoietic mesenchymal stem cells serve as a superior source. J. Cell. Biochem. 99:1132–1147; 2006.